Journal of Geosciences and Geomatics, 2020, Vol. 8, No. 1, 1-8
Available online at http://pubs.sciepub.com/jgg/8/1/1
Published by Science and Education Publishing
DOI:10.12691/jgg-8-1-1

Secondary Enrichment of Ferriferous Pre-Cambrian Quartzites by Meteorical Weathering in South Cameroon

Bidjo Emvoutou Gery Christian[1,3], Ndzie Mvondo Justin[2,3,*], Ngo Bidjeck Louise Marie[3], Ipan Antoinnette[1,3], Ntomb Yvan Demonstel[1,3], Ndong Bidzang Francois[2]

[1]Centre for Geological and Mining Research, P.O. Box: 333, Garoua, Cameroon
[2]Ore Processing Laboratory, Institute for Geological and Mining Research, P.O. Box: 4110Yaounde, Cameroon
[3]Department of Earth Sciences, University of Yaoundé I, P.O. Box: 812, Yaoundé, Cameroon
*Corresponding author: ndziemvondojustin@yahoo.fr

Received November 18, 2019; Revised December 22, 2019; Accepted January 19, 2020

Abstract The meteoric weathering of Precambrian ferriferous quartzites from Meyomessi in southern Cameroon has led, in a humid tropical climate, to the formation of secondary oxidized ores. The weathering profile of the ferriferous quartzites shows from the base to the summit: the bedrock, the saprolites, the gravel horizon and a surface sandy clayey aggregate, ferriferous quartzite is a finely banded rock showing alternating quartz beds and iron oxide beds. The main features of the Meyomessi quartzite geochemistry show that the ferruginous facies are remarkably poor in any element other than Fe and Si. The alteration of the materials shows high Fe, Si, Al, Cr, Zr, Ba, Ga, Nb and Th. Rare earth elements levels are generally low compared to Ce, La and Nd, which are concentrated in upper gravel and sandy-clay levels. The rare earth elements spectrum indicates a positive anomaly in Ce and a negative anomaly in Eu. The results obtained from the calculated balances show a very high enrichment in Al, Ti and K in all the altered materials, low in Si and P in the higher levels and weak in iron in the weathered fragments and in the sandy clay loam level. The losses are total and moderate for all the trace elements, while the rare earths elements are enriched in the soft materials of the whole profile. The iron content in the bedrock (64.9%) versus 68% in the weathered rock fragments (ore), shows that the climatic alteration improves the quality of the ore in the ferruginous fragments by dissolution of the silica and relative concentration iron.

Keywords: *meteorological weathering, ferriferous quartzites, Meyomessi, enrichment*

Cite This Article: Bidjo Emvoutou Gery Christian, Ndzie Mvondo Justin, Ngo Bidjeck Louise Marie, Ipan Antoinnette, Ntomb Yvan Demonstel, and Ndong Bidzang Francois, "Secondary Enrichment of Ferriferous Pre-Cambrian Quartzites by Meteorical Weathering in South Cameroon." *Journal of Geosciences and Geomatics*, vol. 8, no. 1 (2020): 1-8. doi: 10.12691/jgg-8-1-1.

1. Introduction

The ferriferous quartzites of the locality of Meyomessi belong to the tectonic unit of the Ntem complex, which corresponds to the northern margin of the Congo craton. In Cameroon, this Archean domain contains almost all the iron formations identified today [1-5]. There are many iron deposits in the world and pre-Cambrian BIFs are the largest [6]. Archean and Paleoproterozoic rocks are major reservoirs of mineral deposits in the world. In the Ntem complex, the mineral resources associated with Archean and Paleoproterozoic sites are represented by iron whose large reservoirs are banded hematite quartzites or ferruginous quartzites or itabirites [7]. However, despite their abundance, BIFs are a poor iron ore. After their alteration, we can observe their enrichment leading to a rich iron ore, interesting for the industry. This paper aims to understand how the weathering of ferriferous quartzites under humid tropical conditions leads to the formation of secondary oxidized ores.

2. Geological Setting

The study area (Figure 1) belongs to a large litho-structural ensemble of Archean to Paleoproterozoic age [8,9,10]. known as the Ntem complex [11]. This complex corresponds to the northern margin of the Congo craton and is composed of three tectono-metamorphic units: the Ntem unit (3.1-2.1 Ga) [8,12], the Nyong unit and the Ayina unit (2.4-1.8 Ga) [13]. The Ntem unit is dominated by three major groups: a series of basic and ultrabasic rocks and the banded series (granulitic gneiss, leptynites, charnockites and enderbites); a complex of intrusive rocks (syenites, granites, granodiorites, tonalites and trondhjemites) and iron formations (basic rocks and quartzites more or less rich in magnetite) which are organized into different bundles or furrows larding the

basement [4,14-17]. The iron ore deposits currently known in the Ntem complex are in the form of bundles or furrows. The main beams are those of Mezesse, Mbalam, Nkout, Ngoa, Ayina, Ma'an, Abam, Oveng, Mewongo, Nkolbissok, Ngovayang, Eseka [1-5]. Despite the abundance of work on these iron formations in Cameroon, controversies exist as to their origin; Lake Superior for some and Algoma for others.

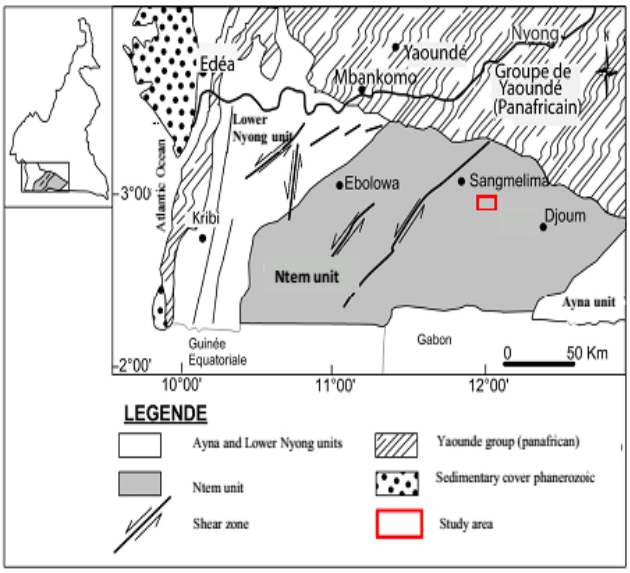

Figure 1. Geological map of South Cameroon (Vicat, 1998)

3. Methodology

In order to study iron ore enrichment processes, a series of wells averaging 85 cm were completed followed by a description of their alteration profile, from the bedrock to the surface. The samples taken were sent to Ireland for geochemical analyzes at the ALS laboratory in Lougrhea. For each sample, a 0.25 g powder is added to a solution of perchloric, nitric and hydrofluoric acid (HClO4, HNO3, and HF). The residue thus obtained is subsequently mixed with one volume of dilute hydrochloric acid (HCl) and the solution obtained is analyzed by ICP-AES (Inductively Coupled Plasma-Atomic Emission Spectroscopy) for the major elements and by ICP-MS (Inductively Couple Plasma-Mass Spectroscopy) for trace elements and rare earth elements. The limit of detection is 0.01% for major elements, between 0.05 and 10 ppm for traces and between 0.01 and 0.5 ppm for rare earth elements.

4. Result

4.1. Weathering Profile

The weathering profile of the ferriferous quartzites can be divided into four, from the base to the top: the bedrock, the saprolite, the gravel horizon, and a sandy clayey aggregate (Figure 2). The bedrock is a ferriferous quartzite whose structures are bedded and folded (Figure 3). It presents an alternation of clear quartz beds and dark beds made up of ferromagnesian minerals. The thicknesses of these beds are very fine more or less differentiated. The rock has a whitish to yellowish gray color and is magnetized. Their mineralogy shows a richness in magnetite and quartz, a smaller amount of martite / hematite secondary minerals, goethite and traces of smectite and gibbsite [2]. The saprolite shows a set of coarse, whitish gray materials with structures similar to those of the parent rock; a non-magnetized weathered material inside which are small bright grains, yellowish and brown spots; a ferruginous material of red color with yellowish spots, small glittery flakes and quartz crystals with friable texture and angular structure; a nodular material of rounded shape, with smooth contours and reddish yellowish color; quartz grouped in clusters, colorless and limpid with angular contours. The transition between these materials is diffuse because the elements are mixed. Also, all of these different materials are bathed in a matrix with a silty texture. The thickness of this horizon is 12 cm. The gravel horizon consists of small gravel, the size of which is less than one centimeter. Dark red in color, the matrix set illustrates a sandy-loamy texture as well as small, shiny white quartz grains. The thickness is 32 cm for this horizon. Dark sandy clay-sandy horizon due to the presence of organic matter. It has neither stain nor concretion and has a sandy-clay texture. The matrix consists of grass roots of varying diameter and size. It is fragile, loose and porous with a thickness of 20 cm (Figure 2).

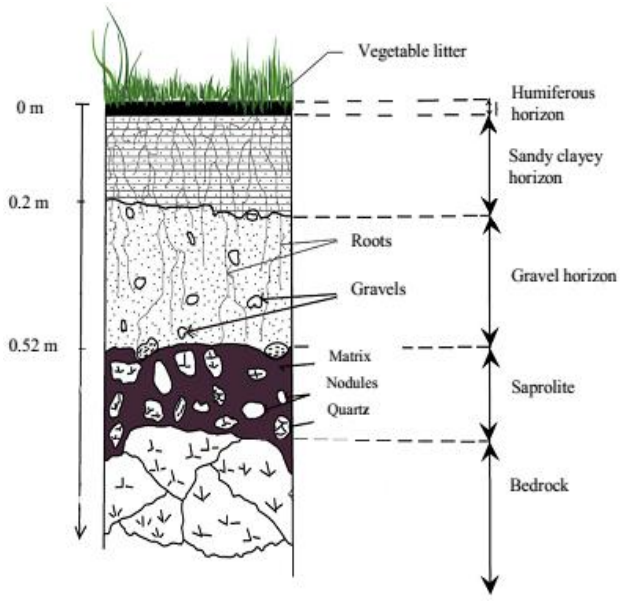

Figure 2. Weathering profile sketch of study area

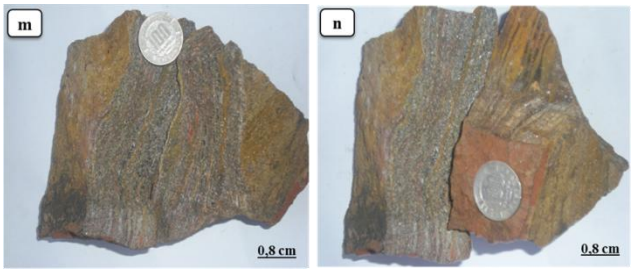

Figure 3. Photograph of ferriferous quartzites of Nkolmvom showing macroscopics characters

Table 1. Major Element Contents (wt.%) in Weathering Profile. d. l.: detection limit

Weathering Profil & Samples		Bedrock	Saprolite		Gravels Horizon	Sandy Clayey Horizon
			Matrix	Altered Rock Fragments		
		RMME	EM3	EM3N	EM2	EM1
Depth (m)		**0.85**	**0.65**	**0.65**	**0.52**	**0.2**
Oxydes	**d. l.**	**Contents in %**				
SiO_2	0.01	34.3	34.1	14.6	39.5	40
Al_2O_3	0.01	0.4	14.5	8.61	20.2	18.85
Fe_2O_3	0.01	64.9	41.7	68	26	26.3
CaO	0.01	-	0.01	-	0.01	0.11
MgO	0.01	0.2	0.1	0.03	0.15	0.15
Na_2O	0.01	0.01	0.01	-	0.01	0.01
K_2O	0.01	0.01	0.09	0.01	0.16	0.17
TiO_2	0.01	0.01	0.48	0.17	0.75	0.72
MnO	0.01	0.11	0.04	0.05	0.03	0.04
P_2O_5	0.01	0.16	0.14	0.19	0.14	0.13
LOI	0.01	0.33	9.55	9.19	12.65	13.9
Total	0.13	100.47	100.76	100.88	99.64	100.41

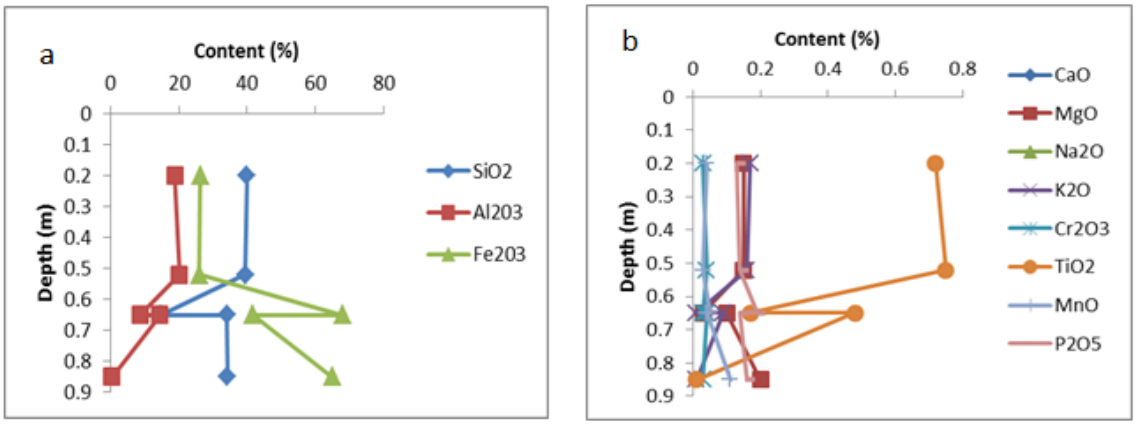

Figure 4. Behaviour and geochemical trends of major elements along the loose materials of the profile

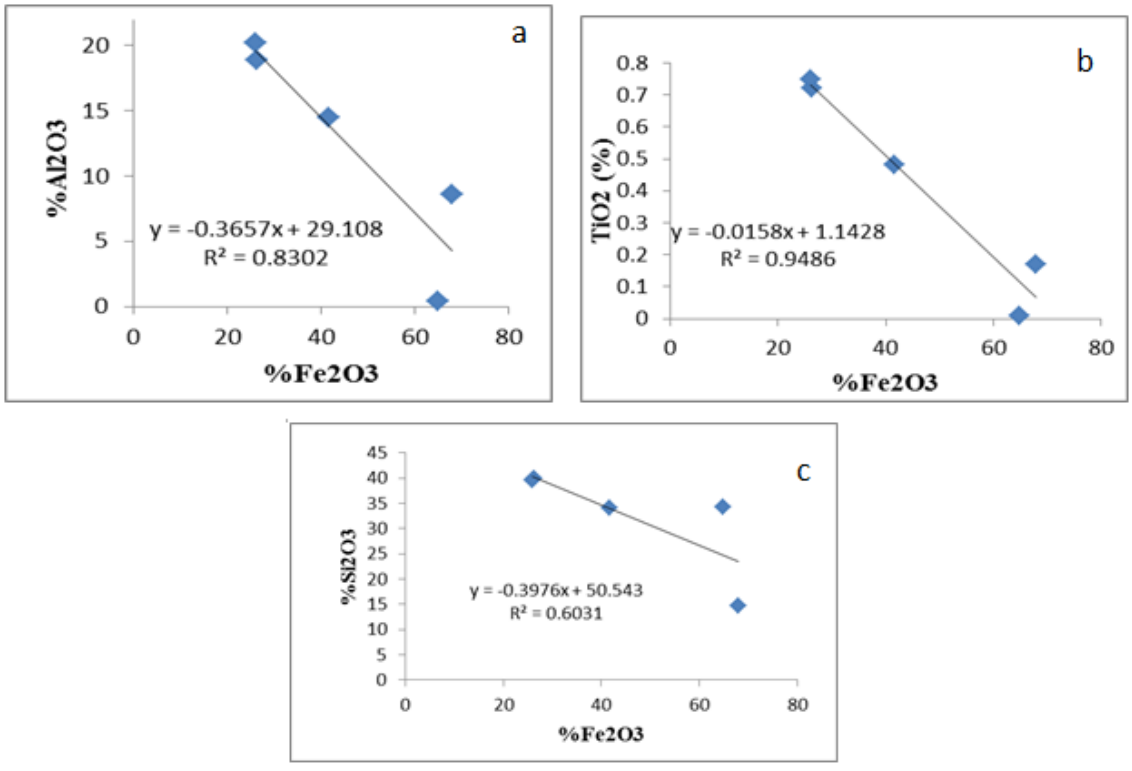

Figure 5. Major elements correlations

4.2. Geochemistry of the Ferriferous Quartzite and Its Weathering Mantle

4.2.1. Major Elements

The results of the geochemical analyzes contained in Table 1 make it possible to follow the evolution of the major elements along the alteration profile (Figure 4 a and b). The silica shows a content of 34.3% in the source rock. This content decreases considerably in the altered rock fragments, then increases and varies little along the profile. Alumina as it is in trace (0.4%) in the bedrock, it sees its content oscillate along the profile, is 14.5% in the matrix, 8.61% in the altered fragments and 18.85% in the sandy-clay horizon. Iron, on the other hand, has a content of 64.9% in the source rock and 68% in the rock fragments altered. Calcium, magnesium, sodium, potassium, manganese and phosphorus are in trace along the alteration profile and vary gradually but very little. On the other hand, titanium although being in trace shows contents a little higher than the other elements in this category. Its content is 0.01% in the source rock; it increases by 0.48% in the matrix, then decreases by 0.17% in the altered rock fragments and increases again by 0.72% on the horizon sandy clay. The correlation diagrams of the major elements of the alteration materials (Figure 5 a, b and c) show that the iron content increases when those of alumina, titanium and silica decrease. As a result, we can conclude that the correlations between iron and alumina, titanium and silica are essentially negative.

4.2.2. Trace Elements and Rare Earth Elements

The geochemical data contained in Table 2 made it possible to follow the evolution of the trace elements along the alteration profile Figure 6 (a, b and c). Chromium has a content of 240 ppm in ferriferous quartzite. This content is almost constant from the bedrock to the gravel horizon, then decreases by 10 ppm in the sandy-clay horizon. Zirconium, meanwhile, has a content of 287 ppm in the bedrock; which content decreases considerably along the profile until reaching 2 ppm at the sandy-clay horizon. Gallium, niobium and rubidium have respective contents of 27.8 ppm; 26.9 ppm and 26.2 ppm in the bedrock, which gradually decrease along the profile. Barium and thorium have respective contents of 46.5 ppm and 46.9 ppm in the bedrock. These levels decrease in the altered rock fragments and increase respectively by 30.7 ppm and 40.2 ppm in the gravel horizon. On the sandy-clay horizon, while the barium has a high content (58.7 ppm) the thorium is in trace (0.64 ppm). Vanadium reveals a content of 80 ppm in ferriferous quartzite. This content gradually decreases along the profile to reach a value of 6 ppm in the sandy-clay horizon. Cs, Hf, Sn, Sr and Ta have the same evolution. Their respective contents of 2.18 ppm, 7.4 ppm, 9 ppm, 19.6 ppm and 1.1 ppm in the ferriferous quartzite decreases progressively from the base to the saprolite, then increases on the gravel horizon to reduce again to the sandy-clay horizon until reaching a value lower than that of the limit of detection. Despite its low grade, uranium gradually increases from ferriferous quartzite to saprolite, and decreases by 0.47 ppm in the sandy-clay horizon. Rare earth elements (Table 3) generally follow the same behavior. Their high levels in ferriferous quartzite decrease in the altered rock fragments, and progressively increase to the sandy-clay horizon (Figure 7 a and Figure 7b). We also note that the highest values are on the gravel horizon and the sandy-clay horizon. The rare earth elements normalization of the alteration materials is carried out with respect to the ferriferous quartzites (parent rock: RMME): Their spectra (Figure 8) show a profile that gradually increases from lanthanum to lutetium with a positive Ce anomaly and a negative Eu anomaly. Many studies show that in a supergene environment under an equatorial climate, several elements are considered immobile and therefore more resistant to redistribution of elements due to weathering phenomena [18,19]. This work proposes several methods for the evaluation of element redistributions such as: Al, Ti, Zr, Nb, Hf, Ta, Th and Y which have often been used for the calculation of the balances. For the evaluation of the gains and losses in each element during the weathering of the Meyomessi ferriferous quartzite, the results obtained from the calculated balances show a very high enrichment in Al, Ti and K in all materials weathered, low in Si and P in the upper and lower levels of iron in the weathered fragments and in the loose sandy-clay level (Table 4); (Figure 9). Losses are moderate to total for all trace elements except uranium (U), which is weakly accumulated in weathered fragments (Table 5); (Figure 10); while rare earth elements are enriched in the loose materials of the whole profile (Table 6); (Figure 11). The weathered fragments are depleted in light rare earth elements except Samarium (Sm) but enriched in heavy rare earth elements except Gadnium (Gd).

Table 2. Content in ppm of Trace Elements in Weathering Materials

Weathering profil & Samples	Bedrock	Saprolite			Gravels Horizon	Sandy Clayey Horizon
		Matrix	Altered Rock Fragments			
	RMME	EM3	EM3N		EM2	EM1
Depth (m)	0.85	0.65	0.65		0.52	0.2
Trace Elements	d. l.	Content in ppm				
Ba	0.5	46.5	42.1	29.1	30.7	58.7
Cr	10	240	240	240	240	230
Cs	0.01	2.18	1.87	0.08	1.21	0.07
Ga	0.1	27.8	24.8	13.2	20.5	3.7
Hf	0.2	7.4	6.8	2	4.3	<0.2
Nb	0.2	26.9	26.2	7.9	19	0.4
Rb	0.2	26.2	22.2	1.2	12.6	0.9
Sn	1	9	3	1	8	5
Sr	0.1	19.6	14	3.1	9.3	5.8
Ta	0.1	1.1	0.9	0.4	1.1	0.1
Th	0.05	46.9	45.5	34	40.2	0.64
U	0.05	5.99	5.9	7.24	5.23	0.47
V	5	80	77	45	65	6
W	1	2	2	2	1	-
Y	0.5	10.8	10.8	7	8	6.2
Zr	2	287	265	72	176	2

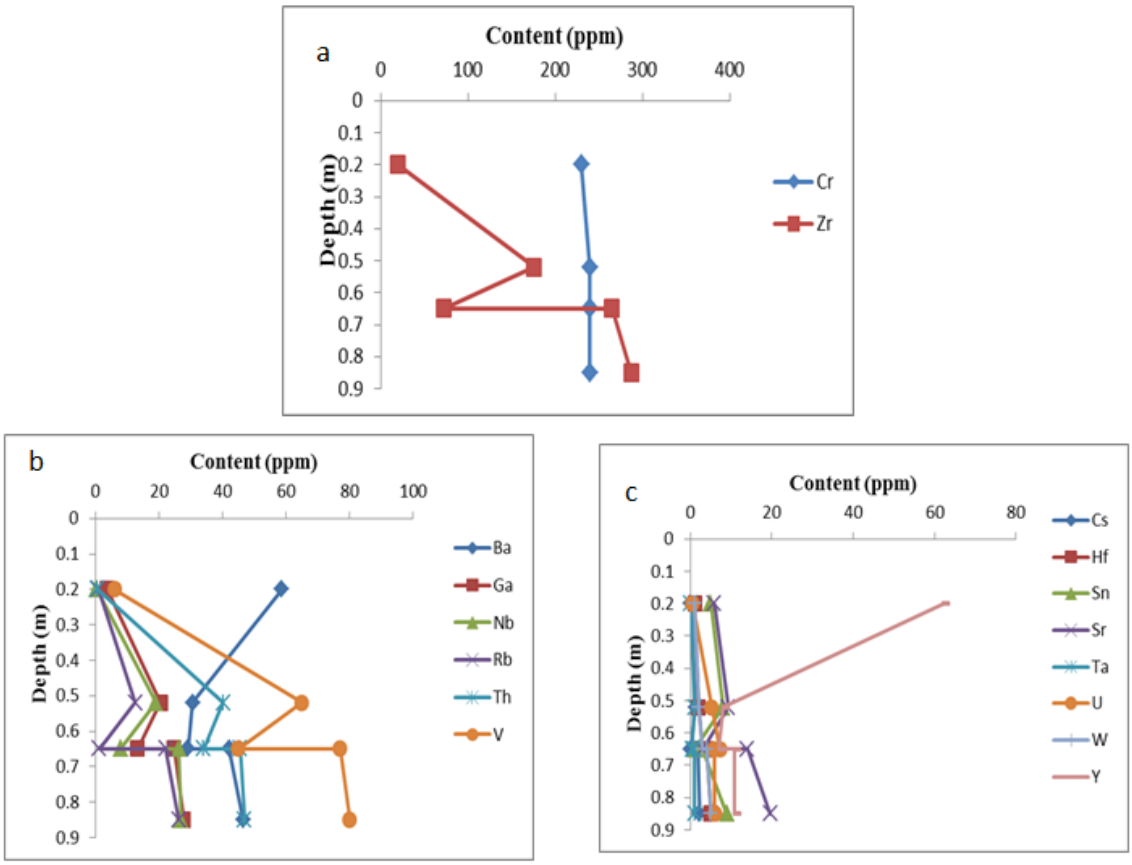

Figure 6. Behaviour and geochemical trends of trace elements along the loose materials of the profile

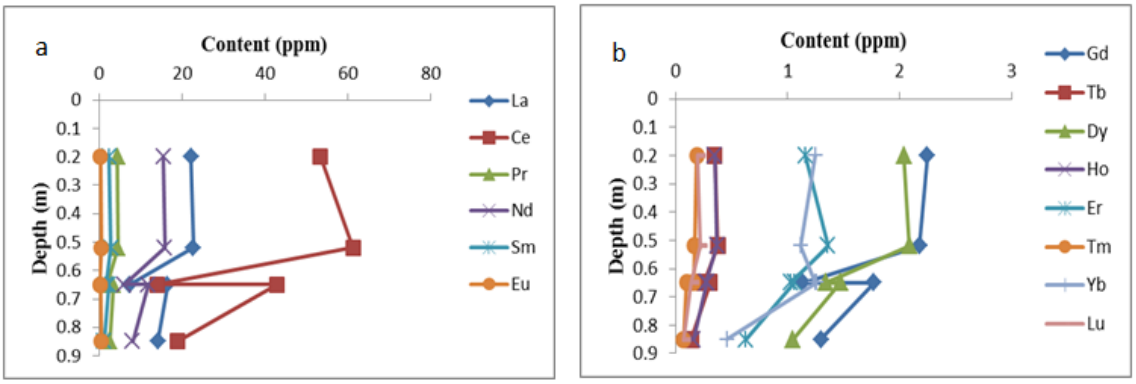

Figure 7. Behaviour and geochemical trends of REE along the loose materials of the profile

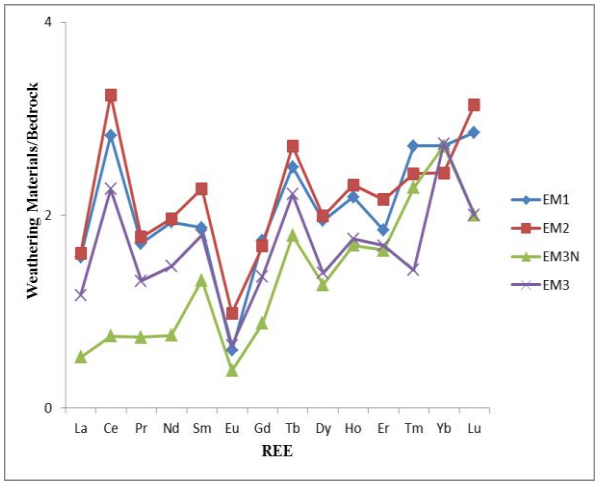

Figure 8. Parent rock normalized for REE_s of weathering materials

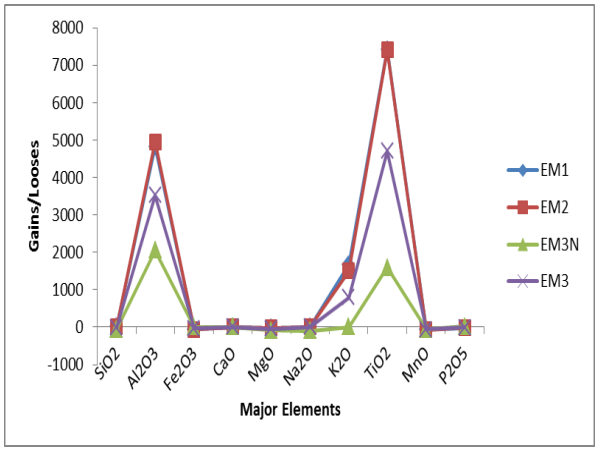

Figure 9. Gains and looses diagram of major elements along weathering profile

Table 3. Content in ppm of REE in Weathering Materials

Weathering Profil & Samples	Bedrock	Saprolite		Gravels Horizon	Sandy Clayey Horizon
		Matrix	Altered Rock Fragments		
	RMME	EM3	EM3N	EM2	EM1
Depth (m)	0.85	0.65	0.65	0.52	0.2
REE	Content (ppm)				
La	14.5	16.6	7.5	22.8	22.2
Ce	18.9	42.9	14.1	61.3	53.4
Pr	2.61	3.44	1.91	4.62	4.45
Nd	8.1	11.9	6.1	15.9	15.6
Sm	1.29	2.31	1.71	2.93	2.41
Eu	0.57	0.37	0.22	0.56	0.34
Gd	1.3	1.77	1.14	2.18	2.25
Tb	0.14	0.31	0.25	0.38	0.35
Dy	1.05	1.47	1.34	2.09	2.04
Ho	0.16	0.28	0.27	0.37	0.35
Er	0.63	1.06	1.03	1.36	1.16
Tm	0.07	0.1	0.16	0.17	0.19
Yb	0.46	1.26	1.25	1.12	1.25
Lu	0.07	0.14	0.14	0.22	0.2
ΣREE	49.87	83.91	37.12	116	106.19
ΣLREE	45.97	77.52	31.54	108.11	98.4
ΣHREE	3.88	6.39	5.58	7.89	7.79
ΣLREE/ΣHREE	11.84	12.13	5.65	13.70	12.63
$(La/Yb)_N$	20.97	8.94	4.07	13.82	12.06
Ce/Ce*	0.75	1.37	0.9	1.44	1.3
Eu/Eu*	1.34	0.55	0.48	0.67	0.44

$(La/Yb)_N = (La_{rock}/La_{chondrite})/(Yb_{rock}/Yb_{chondrite})$
$Ce/Ce^* = (Ce_{rock}/Ce_{chondrite})/(La_{rock}/La_{chondrite})^{1/2}(Pr_{rock}/Pr_{chondrite})$
$Eu/Eu^* = (Eu_{rock}/Eu_{chondrite})/(Sm_{rock}/Sm_{chondrite})^{1/2}(Gd_{rock}/Gd_{chondrite})^{1/2}$.

Table 4. Gains and Looses Percentage of Major Elements

Weathering Profil & Samples	Saprolite		Gravels Horizon	Sandy Clayey Horizon
	Matrix	Altered rock fragments		
	EM_3	EM_3N	EM_2	EM_1
Depth (m)	0.65	0.65	0.52	0.2
Major Elements (%)	Gains and Looses %			
SiO_2	-0.58	-57.43	15.16	21.68
AL_2O_3	3525	2052.5	4950	4817.39
Fe_2O_3	-35.74	4.77	-59.93	57.71
CaO	-	-	-	-
MgO	-50	-85	-25	-21.73
Na_2O	0	-100	0	4.34
K_2O	800	0	1500	1673.91
TiO_2	4700	1600	7400	7413.04
MnO_2	-63.63	-54.54	-72.72	-62.05
P_2O_5	-12.5	18.75	12.5	62.05

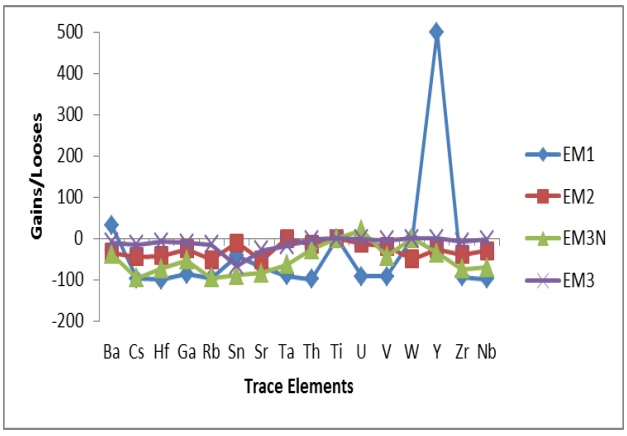

Figure 10. Gains and looses diagram of trace elements along weathering profile

Table 5. Gains and looses percentage of trace elements

Weathering Profil & Samples	Saprolite		Gravels Horizon	Sandy Clayey Horizon
	Matrix	Altered Rock Fragments (nodules)		
	EM_3	EM_3N	EM_2	EM_1
Thickness (m)	0.65	0.65	0.52	0.2
Trace elements	Gains and Looses %			
Ba	-9.46	-37.41	-33.91	31.72
Cs	-14.22	-96.33	-44.49	-96.64
Hf	-8.10	-72.97	-41.89	-100
Ga	-10.79	-52.51	-26.25	-86.11
Nb	-2.60	-70.63	-29.36	-98.44
Rb	-15.26	-95.41	-51.90	-96.41
Sn	-66.67	-88.89	-11.11	-42.02
Sr	-28.57	-84.18	-52.55	-69.12
Ta	-18.18	-63.63	0	-90.51
Th	-2.98	-27.50	-14.28	-98.57
Ti	-	-	-	-
U	-1.50	20.86	-12.68	-91.81
V	-3.75	-43.75	-18.75	-92.17
W	0	0	-50	-
Y	0	-35.18	-25.92	499.03
Zr	-7.66	-74.91	-38.67	-92.72

Table 6. Gains and looses percentage of REE

Weathering Profil & Samples	Saprolite		Gravels Horizon	Sandy Clayey Horizon
	Soil Materials	Weathering Materials (nodules)		
	EM_3	EM_3N	EM_2	EM_1
Thickness (m)	0.65	0.65	0.52	0.2
REE	Gains and Looses %			
La	16.90	-47.18	60.56	63.13
Ce	126.98	-25.39	224.33	194.82
Pr	31.80	-26.81	77.01	77.91
Nd	91.46	-24.69	96.29	100.96
Sm	79.06	32.55	127.13	94.94
Eu	-35.08	-61.40	-1.75	-37.75
Gd	36.15	-12.30	67.69	80.60
Tb	121.42	78.57	171.42	160.86
Dy	40	27.61	99.04	102.73
Ho	75	68.75	131.25	128.06
Er	68.25	63.49	115.87	92.13
Tm	42.85	120.57	142.85	183.22
Yb	173.91	171.73	143.47	183.55
Lu	100	100	214.20	198.13

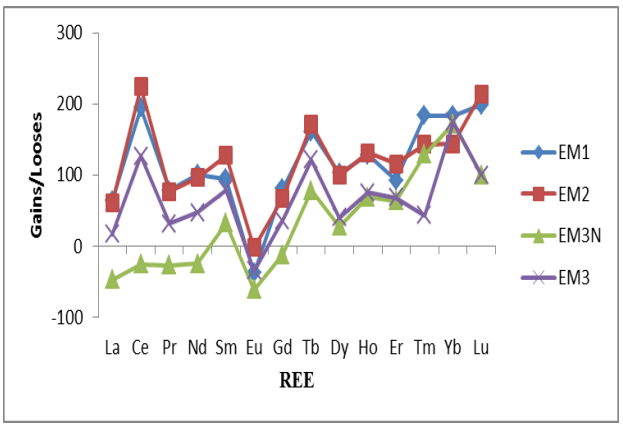

Figure 11. Gains and looses diagram of REE along weathering profile

5. Discussion

The geochemical study of Meyomessi ferriferous quartzites shows a high concentration of Si and Fe, respectively 40% and 68%. As for the rare earth elements, the contents are weak with the exception of Cerium, lanthanum and neodymium which present significant contents. The rare earth element spectrum of chondrite normalized ferriferous quartzite has rare earth elements fractionated and enriched in LREE with respect to HREE. These results are consistent with those obtained for the iron-bearing quartzites of the rest of the Ntem complex [1,2,3,4]. The rare earth elements spectra show a positive anomaly in Ce and a negative anomaly in Eu; the opposite is true in the ferriferous quartzites of Njweng [20]. Thus, the negative Eu anomaly in the Meyomessi samples is due as Reference [21] demonstrates to Abi é é-Yendjock, to the absence of plagioclase in the genesis of these rocks. The weathering material developed at the expense of Meyomessi ferriferous quartzites is ferralitic, yellowish brown to reddish in color and not very thick. Reference [21] shows that the weathering profiles developed on basic and ultrabasic rocks at Abi é é-Yendjock are of low thickness. They have a reduced number of weathering levels and in particular the absence of a ferruginous cuirass level. At Abi é é-Yendjock, the weathering is a ball, it is cortical, centripetal and early whereas that which affects the basic rocks of the Ntem group, to which the study area belongs, is slab or fragments which gradually and slowly reduce to the upper horizons. These fragments are no longer magnetized like the original rock, which reveals that the magnetite contained in the ferriferous quartzite would have been oxidized into hematite known as non-magnetized iron ore. According to Reference [22], kaolinite is formed directly and immediately on very rich quartz materials such as sandstones and alkaline granites [23]. The neoformation of kaolinite is inhibited by a low availability of Si which is either evacuated by excellent lateral and vertical drainage, or precipitates as free silica. The excess of alumina present in the soil then crystallizes in the form of gibbsite. This low availability of Si, which slows the neoformation of kaolinite, also favors the presence of iron oxyhydroxides which have a high nickel retention capacity in the soil [24,25]. The high levels of SiO2, Al2O3 and Fe2O3 testify to the neoformation of clay minerals by recombination of silica and alumina by the monosilitization process; and the neoformation of iron oxyhydroxides by the ferrallitization process. Several authors have shown that rare earth elements are fractionated during the weathering process, residual products are enriched in LREE and poor in HREE [26,27]. Cerium is the most abundant of REEs in weathering materials, followed by lanthanum and neodymium. They are concentrated in all levels of the weathering profile. The positive anomalies observed in cerium are systematic and often located at the top of the saprolite, below the iron oxide accumulation zone [28]. The cerium appears in the solutions in the form of Ce3 + and then of Ce4 + under the oxidation conditions in which it precipitates in the form of insoluble CeO2 [29,30]. It is either absorbed in iron oxides in association with phosphates [31], either incorporated in ferro-manganese chippings [32], or absorbed at the clay exchange sites [33,34]. The negative Eu anomaly may be due to oxidation conditions in an environment and / or in the absence of sulphides and plagioclases [35]. Levels of Fe (68%), P (0.19%) and U (7.24 ppm) are higher in weathered fragments that have low concentrations of Al, Si and other elements at the same time. The precipitation of secondary phosphate minerals is known to play an important role in the immobilization of trace elements within developed and water-saturated alteration profiles [36]. Phosphates are also known as absorption immobilizers of uranium [37] or as precipitators of phosphate minerals carrying uranium [38].

6. Conclusion

This article has shown how tropical climate meteorological action enhances iron richness in oxidized rock fragments from the weathering of ferriferous quartzites. The results obtained in the Meyomessi Precambrian ferriferous Quartzite Well Disturbance profiles in southern Cameroon clearly show that during weathering, the weathering materials are enriched in Fe, Si, Al, Cr, Zr. , Ba, Ga, Nb and Th. The Fe, P and U contents are higher in the weathered fragments which have low concentrations of Al, Si and other elements at the same time and which constitute the main iron ore.

Acknowledgments

The authors thank the Lougrhea laboratory of the ALS group for the quality of the analyzes and the reviewers who contributed to the improvement of this article.

References

[1] Chombong, N.N., Suh, C.E., 2013. 2883 Ma commencement of BIF deposition at the northern edge of Congo craton, southern Cameroon: new zircon SHRIMP data constraint from metavolcanics. Episodes 36, 47-57.

[2] Ganno S., Ngnotue, T., Kouankap Nono, G.D., Nzenti, J.P., Notsa, F.M., 2015. Petrology and geochemistry of the banded iron-formations from Ntem complex greenstones belt, Elom area, Southern Cameroon: implications for the origin and depositional environment. Chem. Erde 75, 375-387.

[3] Ilouga, C.D.I., Suh, C.E., Ghogomu, R.T., 2013. Textures and rare earth elements composition of Banded Iron Formations (BIF) at Njweng prospect, Mbalam Iron Ore District, Southern Cameroon. Int. J. Geosci. 4, 146-165.

[4] Ndong Bidzang Francois, Sobdjou Kemteu Christel, Mero Yannah, Ntomba Martial Sylvestre, Nzenti Jean Paul, Mvondo Ondoa Joseph. Origin and Tectonic Framework of the Ngovayang Iron Massifs, South Cameroon. Science Research. Vol. 4, No. 1, 2016, pp. 11-20.

[5] Nsoh, F.E., Agbor, T.A., Etame, J., Suh, E.C., 2014. Ore-textures and geochemistry of the Nkout iron deposit South East Cameroon. Sciences. Technol. D év. 15, 43-52.

[6] Ramana ïlou, E(1989). Genèse d'un gisement latéritique. Evolution superg ène des itabirites prot érozo ïques de la mine de Capanema (Minas Gerais, Br ésil). Th. Doc., Univ. Poitiers, 183p.

[7] Eno Belinga S. M. (1986). Il y'a 600 millions d'années…métaux, non m étaux et substances utiles du Cameroun. C.E.P.E.R., 128p.

[8] Lasserre M. et D. Soba (1976). Migmatisation d'âge panafricain au sein des formations Camerounaises appartenant à la zone mobile de l'Afrique Centrale. C.R. Somm. Soc. Géol. Fr., 2p. 64-68.

[9] Toteu, S. M., Van Schmus, W. R., Penaye, J., and Nyobé, J. B. (1994). U-Pb and Sm-Nd evidence of eburnean and pan African high grade metamorphism in cratonic rock of southern Cameroon. Precambrian Research Vol. 67: 321-347.

[10] Shang, C.K., Liégeois, J.-P., Satir, M., Nsifa, E.N., 2010. Late Archaean high-K granite geochronology of the northern metacratonic margin of the Archaean Congo craton. Southern Cameroon: evidence for Pb-loss due to non-metamorphic causes. Gondwana Research 18, 337-355.

[11] Owona, S. Mvondo Ondoa, J. Ratschbacher, L. Mbola Ndzana, S.P. Tchoua, M.F. & Ekodeck, G.E. 2011. The geometry of the Archean, Paleo- and Neoproterozoic tectonics in the Southwest Cameroon. Comptes Rendus Geosciences, 343: 312-322.

[12] Shang, C.K., Siebel, W., Satir, M., Chen, F., Mvondo Ondoua, J., 2004. Zircon Pb–Pb and U–Pb systematics of TTG rocks in the Congo Craton: constraints on crust formation, magmatism, and Pan-African lead loss. Bulletin of Geosciences 79 (4), 205-219.

[13] Ledru, P., Johan, V., Mile ́si, J.P., Tegyey, M., 1994. Markers of the last stages of the Palaeoproterozoic collision: evidence for a 2 Ga continent involving circum-South Atlantic provinces. Precamb. Res. 69,169-191.

[14] S. M. Ntomba, F. Ndong Bidzang, J. E. Messi Ottou, Fran çois, J. Goussi Ngalamo, D. Bisso, Christelle R. Magnekou Takamte, J. Mvondo Ondoa. Phlogopite compositions as an indicator of both the geodynamic context of granitoids and the metallogeny aspect in Memve'ele Archean area, northwestern Congo craton. Journal of African Earth Sciences 118 (2016) 231-244.

[15] Nsifa, N. E., Tchameni, R., Nédélec, A., Siqueira, R., Pouclet, A., Bascou, J., 2013. Structure and petrology of Pan-African nepheline syenites from the South West Cameroon; Implications for their emplacement mode, petrogenesis and geodynamic significance. Journal of African Earth Sciences 87, 44-58.

[16] Nédélec, A., Nsifa, E.N., Martin, H. (1990). Major and trace element geochemistry of the Archean Ntem plutonic complex (South Cameroon) :petrogenesis and crustal evolution provenance of detritus for the Nyong Group. Precambrian Research Vol.47: 35-50.

[17] Nedelec, A. et Nsifa, E. N., 1987. Le complexe du Ntem (Sud-Cameroun): une série tonalito-trondhjémitique archéen typique. Cur. Reaserch. In Africa. Earth Sc. Matheis and Schandelmeier (eds), pp 3-6.

[18] Kurtz, A.C., Derry, L.A., Chadwick, O.A., Alfano, M.J., 2000. Refractory element mobility in volcanic soils. Geology 28 (8), 683-686.

[19] Braun, J.-J., Viers, J., Drupre, B., Polve, M, Ndam, J.R., Muller, J.-P. (1993). Solid/liquid REE fractionation in the lateritic system of Goyoum, East Cameroun: The Geochim. Cosmochim. Acta 62, 2, 273-299.

[20] Ilouga, D. C. I., Suh C. E., Tanwi G. R. (2013). Textures and Rares Earth Elements Composition ozvf Banded Iron Formations (BIF) at Njweng Prospect, Mbalam Iron Ore District, Southern Cameroon. International Journal of Geosciences, 4, pp146-165.

[21] Ngo Bidjeck, L.M., 2004. L'altération des roches basiques et ultrabasiques du Sud-Ouest Cameroun et ses implications métallogéniques. Cas du complexe d'Abiété-Yenjok. Thèse de Doct. /Ph.D, Univ. de Yaoundé I, 267 p.

[22] Duchaufour, P. (1978). Ecological Atlas of Soils of the World. 1978 pp.178 pp.

[23] Blot A, C m M, Leprun JC et Pion JC, 1976, Premier bilan des études géologiques et pédologiques d'un corps ultra basique et de son contexte : Koussâne au Sénégal Oriental . CA. ORSTOM sér. Geel., vol VI11 , n02,113-145.

[24] Manikyamba, C., Naqvi, S.M., 1995. Geochemistry of Fe–Mn formations in the Archean Sandur schist belt, India: mixing of clastic and chemical processes at a shallow shelf. Precambrian Res. 72, 69-95.

[25] Pelletier, B. (1983). Localisation du nickel dans les minerais «garnieritiques » de Nouvelle -Calédonie. Sci. Geol. Mem, 73. P173-183.

[26] Duddy, I. R. (1980). Redistribution and fractionation of rare earth and other elements in weathering profile. Chem. Geol. 30, 363-381.

[27] S.E. Topp, B. Salbu, E. Roaldset, P. Jørgensen, 1984. Vertical distribution of trace elements in laterite soil (Suriname). Chemical Geology Pages 159-174.

[28] Braun I (1999) Generation of leucogranites in the Kerala Khondalite Belt, southern India. Phys Chem Earth (A) 24: 281-287.

[29] Jean Braun; Christopher Beaumont, 1989. A physical explanation of the relation between flank uplifts and the breakup unconformity at rifted continental margins. Geology (1989) 17 (8): 760-764.

[30] Brokins, D.G. (1988). Eh-Ph diagrams for Geochemistry, Springer-Verlang, Berlin Heidelberg.

[31] Leleyter, L., Probst, J.L., Depetris, P., Haida, S., Mortatti, J., Rouault, J., Samuel, J. (1999). REE redistribution and labile fractions C.R. Acad. Sci.ParisSer. IIa 329. 45-52.

[32] Piper, 1974. Rare earth elements in the sedimentary cycle: A summary. Chemical Geology Pages 285-304.

[33] Aagaard, P. (1974). Rare earth absorption on clay minerals.Bull. Groupe Fr. argiles 26, 193-199.

[34] E. Roaldset, 1974. Lanthanide distributions in clays. Bull. Groupe franc. Argile. tXXVI, pp. 201-209.

[35] Matthew I. Leybourne, Eion M. Cameron, 2006. Composition of Soils and Ground Waters at the Pampa del Tamarugal, Chile: Anatomy of a Fossil Geochemical Anomaly Derived from a Distant Porphyry Copper Deposit. Economic Geology (2006) 101 (8): 1569-1581.

[36] Braun, J.-J., Viers, J., Dupre ́, B., Polve, M., Ndam, J., Muller, J.P., 1998.Solid/liquid REE fractionation in the lateritic system of Goyoum, East Cameroon: the implication for the present dynamics of the soil covers of the humid tropical regions. Geochim. Cosmochim. Acta 62 (2), 273-299.

[37] Mc Murry Je; Miller Dd, 1983. Synthesis Of Isocaryophyllene By Titanium-Induced Keto Ester Cyclization. Tetrahedron Letters; Issn 0040-4039; Gbr; Da. 1983; Vol. 24; No 18; Pp. 1885-1888; Bibl. 8 Ref.

[38] James L. Jerden Jr, A.KSinha, 2003. Phosphate based immobilization of uranium in an oxidizing bedrock aquifer. Applied Geochemistry, Elsevier Science Volume 18, Issue 6, June 2003, Pages 823-843.